



Discovery of dual inhibitors targeting both HIV-1 capsid and human cyclophilin A to inhibit the assembly and uncoating of the viral capsid

Jiebo Li^a, Zhiwu Tan^a, Shixing Tang^b, Indira Hewlett^b, Ruifang Pang^a, Meizi He^a, Shanshan He^a, Baohe Tian^a, Kan Chen^a, Ming Yang^{a,*}

^aState Key Laboratory of Natural and Biomimetic Drugs, Peking University, PO Box 261, Beijing 100191, China

^bCenter for Biologics Evaluation and Research, Food and Drug Administration, Bethesda, MD 20892, USA

ARTICLE INFO

Article history:

Received 21 January 2009

Revised 19 February 2009

Accepted 21 February 2009

Available online 3 March 2009

Keywords:

HIV-1

Capsid

Cyclophilin A

Assembly

Disassembly

Dual inhibitor

ABSTRACT

HIV-1 assembly and disassembly (uncoating) processes are critical for the HIV-1 replication. HIV-1 capsid (CA) and human cyclophilin A (CypA) play essential roles in these processes. We designed and synthesized a series of thiourea compounds as HIV-1 assembly and disassembly dual inhibitors targeting both HIV-1 CA protein and human CypA. The SIV-induced syncytium antiviral evaluation indicated that all of the inhibitors displayed antiviral activities in SIV-infected CEM cells at the concentration of 0.6–15.8 μ M for 50% of maximum effective rate. Their abilities to bind CA and CypA were determined by ultraviolet spectroscopic analysis, fluorescence binding affinity and PPIase inhibition assay. Assembly studies in vitro demonstrated that the compounds could potently disrupt CA assembly with a dose-dependent manner. All of these molecules could bind CypA with binding affinities (K_d values) of 51.0–512.8 μ M. Fifteen of the CypA binding compounds showed potent PPIase inhibitory activities (IC_{50} values < 1 μ M) while they could not bind either to HIV-1 Protease or to HIV-1 Integrase in the enzyme assays. These results suggested that 15 compounds could block HIV-1 replication by inhibiting the PPIase activity of CypA to interfere with capsid disassembly and disrupting CA assembly.

© 2009 Elsevier Ltd. All rights reserved.

1. Introduction

Antiretroviral therapy has led to a significant improvement in the prognosis for HIV-1-infected individuals. The currently used anti-HIV-1 drugs target the envelope protein, reverse transcriptase (RT), integrase (IN) and protease (PR), to block HIV-1 infection at the stage of entry, reverse transcription, integration and maturation, respectively.¹ However, new anti-AIDS drugs are urgently needed because of the growing problems of drug resistance and the serious side-effects of the current drugs. Some new compounds that target different viral proteins or various steps of viral life cycles are widely investigated.² However, the assembly and disassembly processes of HIV-1 capsid (CA) protein have received less attention as antiviral drug targets compared to IN, PR and RT.^{3–5}

Recently, several inhibitors that bind to HIV-1 CA had been reported,^{6,7} such as a helical peptide inhibitor⁸ (CAI) that binds between CA CTD(C-terminal domain) helices 8 and 11, and two small molecule inhibitors⁹ (Fig. 1) that insert into a pocket formed at the junction between helices 1, 2, 4 and 7 in the NTD (N-terminal domain) of HIV-1 CA. These inhibitors bind within or adjacent to the third interface and probably disrupt this interaction thereby

inhibiting CA assembly.⁷ Kelly et al. elucidated the binding model of CAP-1 and CA NTD, and found that the interaction between CAP-1 and CA NTD can displace Phe32 from the NTD core and open a deep hydrophobic cavity to the small molecule inhibitor.¹⁰ The aromatic ring of CAP-1 inserts into the cavity, and its urea NH groups form hydrogen bonds with the backbone oxygen of Val59. Recent studies^{11,12} have also shown that several small molecules can bind to the 'saddle' pockets of CypA (pocket A and pocket B)

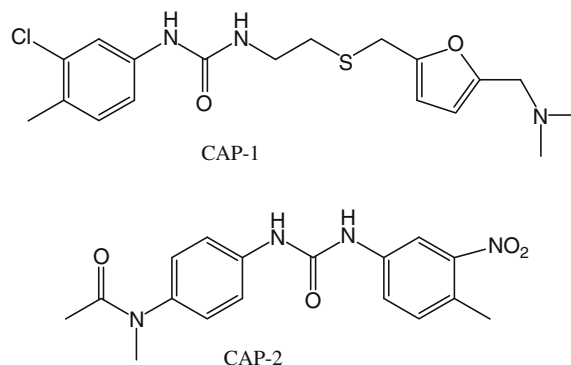


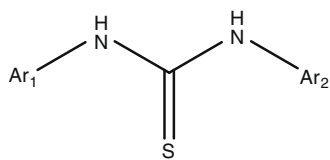
Figure 1. Structures of CAP-1 and CAP-2.

* Corresponding author. Tel.: +86 10 82805264; fax: +86 10 82802724.

E-mail address: yangm@bjmu.edu.cn (M. Yang).

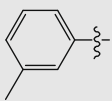
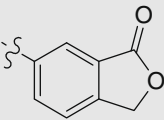
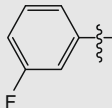
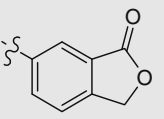
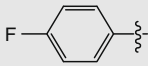
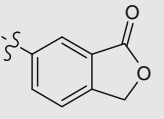
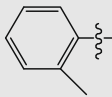
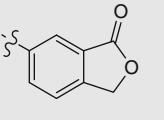
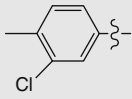
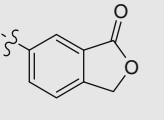
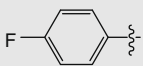
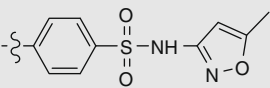
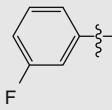
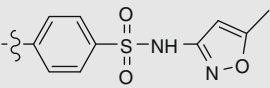
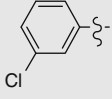
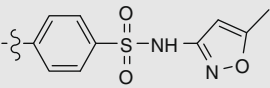
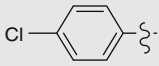
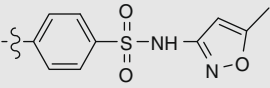
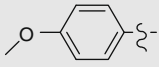
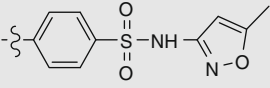
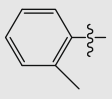
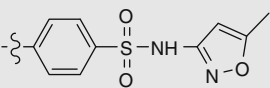
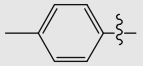
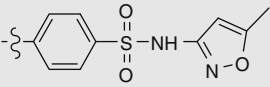
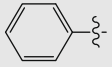
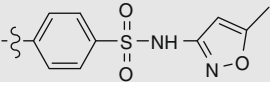
Table 1

Chemical structure, inhibition effect and cytotoxicity of the title compounds on SIV induced syncytium



Entry	Ar ₁	Ar ₂	EC ₅₀ (μM)	TC ₅₀ (μM)	TI (TC ₅₀ /EC ₅₀)
T1			6.3	44.1	7
T2			7.4	26.2	4
T3			5.5	8.43	2
D1			2.3	16.1	7
D2			3.1	38.8	12
D3			4.6	30.8	7
D4			6.2	83.9	14
D5			4.2	86	20
D6			4.7	91.9	20
D7			3.0	24.4	8
D8			6.1	69.1	11

Table 1 (continued)

Entry	Ar ₁	Ar ₂	EC ₅₀ (μM)	TC ₅₀ (μM)	TI (TC ₅₀ /EC ₅₀)
D9			11.6	16.0	1
D10			6.3	60.2	10
D11			15.8	83.7	5
D12			2.8	46.9	17
D13			4.6	18.7	4
D14			6.9	75.4	11
D15			11.6	88.0	8
D16			1.0	91.9	92
D17			4.1	37.8	9
D18			1.5	41.9	27
D19			6.2	48.4	8
D20			9.6	41.4	4
D21			7.5	49.7	7

(continued on next page)

Table 1 (continued)

Entry	Ar ₁	Ar ₂	EC ₅₀ (μM)	TC ₅₀ (μM)	TI (TC ₅₀ /EC ₅₀)
D22			0.9	58.7	66
D23			0.6	74.4	127
D24			4.1	77.5	19
D25			10.8	37.0	3
D26			5.7	19.1	3
D27			2.2	20.9	9
CsA	—	—	NA ^a	—	—

* EC₅₀, concentration required to protect cells against the cytopathogenicity of SIV by 50%.

^a NA, no activity.

and inhibit its activity catalyzing the *cis/trans*-isomerization of the Gly89-Pro90 peptide bond, which facilitates the disassembly of the HIV-1 CA complex. These researches open a new field to find new inhibitor that target HIV-1 CA to disrupt the assembly and/or disassembly process of HIV-1 CA.

Based on the references mentioned above, we initially selected CAP-1 as leading compound to develop new anti-HIV agents. As shown in Table 1, we maintained thiourea scaffold as linker to connect two main groups, Ar₁ and Ar₂. Ar₁ represented a series of substituted phenyl groups; Ar₂ stood for different types of aryl groups. We designed a novel compound with thiourea as the core structure, and a 3-chloro-4-methoxy-phenyl (the activity group of CAP-1) as Ar₁ and a *N*⁴-(2-aminoethyl)-*N*²,*N*²-diethyl-6-methyl-5-nitropyrimidine-2,4-diamine as Ar₂ (**T1**). Secondly, we changed the 3-bromide phenyl instead of 3-chloro-4-methoxy-phenyl to test whether the different kind of phenyl substituent would potentially influence the activity (**T2**). Thirdly, we kept the 3-bromide phenyl and eliminated the nitro-group in pyrimidine to identify the activity of nitro-group (**T3**). Therefore, the biological experiments revealed that the modification of substituted phenyl group could change the inhibiting capability of compounds. However, the introduction of *N*⁴-(2-aminoethyl)-*N*²,*N*²-diethyl-6-methyl-5-nitropyrimidine-2,4-diamine could not improve the activity compared with CAP-1, which inspired us to design new types of assembly inhibitors.

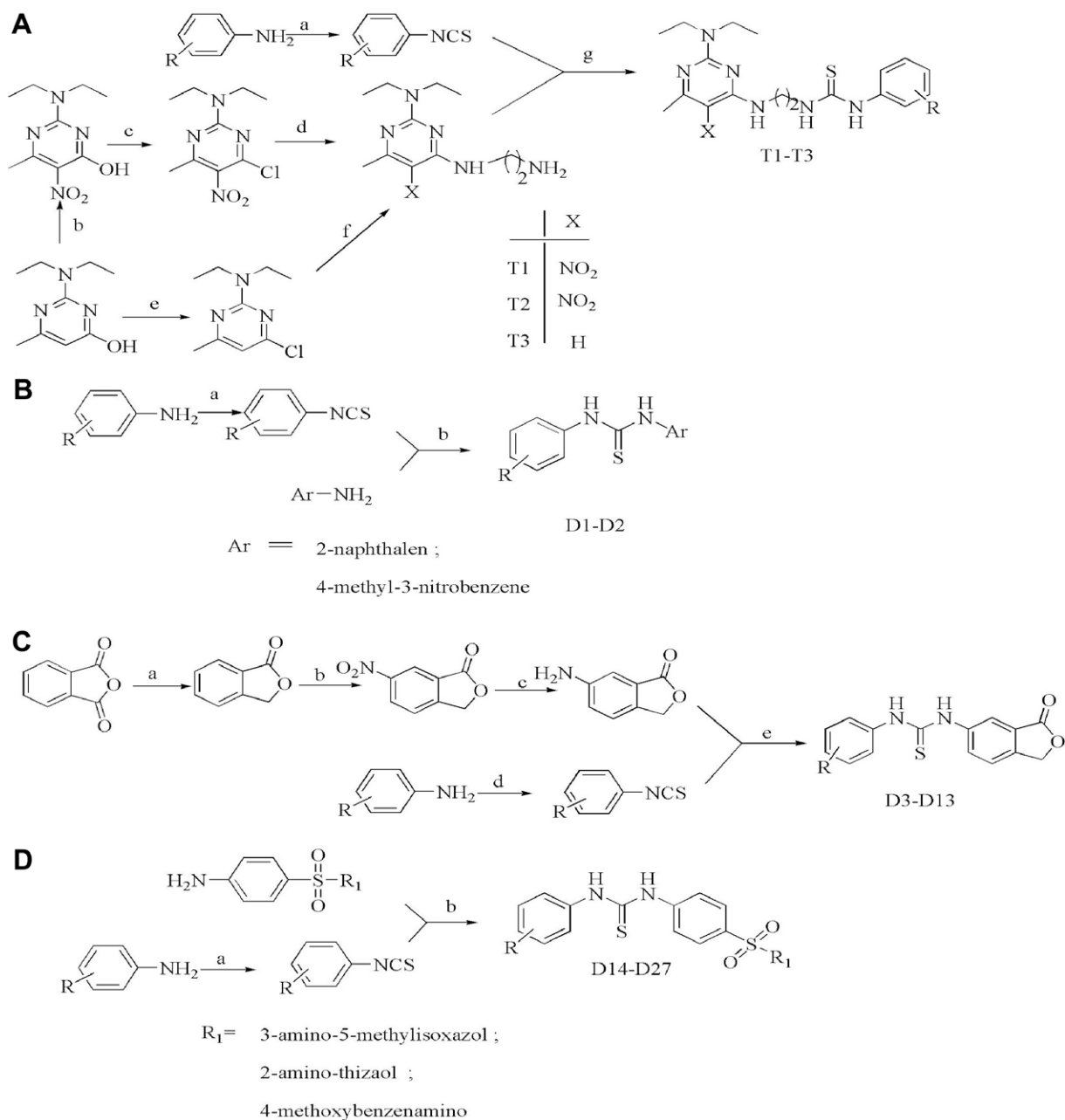
Then, we linked the 3-chloro-4-methyl phenyl of CAP-1 and 3-nitro-4-methyl phenyl of CAP-2 which had been reported as the agents to inhibit CA assembly in vitro with thiourea scaffold. Consequently, the 6-isobenzofuran-1(3*H*)-one was selected to substitute the aromatic nitro group to avoid the cell toxicity. Different

kinds of substitute phenyls (*o*-CH₃, *m*-F, *m*-Cl, *m*-Br, *p*-F, *p*-CH₃, *p*-OCH₃ and *p*-Cl) were introduced to evaluate the influence of anti assembly activity. Then, according to the binding model of CAP-1 and CA had been clearly interpreted⁷, we extrapolated that larger phenyl groups and some hydrogen receptors outside the cavity would form stronger hydrophobic interaction and hydrogen with the protein. As an attempt, we introduced the pharmacophore-sulfamethoxazole segment (**D14–D23**). Finally, the introductions of the 4-methoxybenzene (**D24**) and thiazole (**D25–D27**) instead of isoxazolyl were to investigate the groups' assembly inhibitory.

2. Results and discussion

The routes used for preparation of the title compounds were illustrated in Scheme 1 and the synthetic procedures were explained in Section 4. Thirty compounds were obtained and their MS, ¹H NMR spectroscopy data were provided in Section 4.

As shown in Table 1, we evaluated these thiourea compounds using SIV-induced syncytium assay in CEM cells to test their the concentration for 50% of maximum effect (EC₅₀), concentration for 50% of maximum toxic (TC₅₀) and therapeutic index (TI) values. The thiourea compounds inhibited viral replication with a range of EC₅₀ values from 0.6 μM to 15.8 μM. Compound **D23** showed best EC₅₀ value. Its TI value was also greater than 100. The compounds (**D16**, **D22** and **D23**) which consisted of *meta*-chlorine or bromine mono-substituted phenyl at Ar₁ and sulfamethoxazole group at Ar₂ showed very good antiviral activities (EC₅₀ < 1 μM). Nevertheless, the compounds consisted of *meta*-fluorine substituted phenyl at Ar₁ and sulfamethoxazole group at Ar₂ displayed the weakest antiviral capability (EC₅₀ > 10 μM). As the TRIM5α could interact



Scheme 1. Reagents and conditions: (a) (1) 1,4-diazabicyclo[2,2,2]-octane, CS₂, rt, 12 h, (2) BTC, reflux, 2 h (for two steps); (b) HNO₃, H₂SO₄, rt, 24 h; (c) POCl₃, Me₂NC₆H₄, reflux, 5 h; (d) amine, ethanol, rt, 24 h; (e) POCl₃, reflux, 3 h; (f) 1,2-diaminoethane, ethanol, rt, 26 h; (g) N(C₆H₅)₃, reflux, 5 h; (B) Reagents and conditions: (a) (1) 1,4-diazabicyclo[2,2,2]-octane, CS₂, rt, 12 h, (2) BTC, reflux, 2 h (for two steps); (b) C₂H₅OH, room temperature, 12 h; (C) Reagents and conditions: (a) NaBH₄, CH₃OH, THF; (b) KNO₃, H₂SO₄; (c) SnCl₂, 37% HCl solution, 50 °C; (d) (1) 1,4-diazabicyclo[2,2,2]-octane, CS₂, rt, 12 h, (2) BTC, reflux, 2 h (for two steps); (e) C₂H₅OH, room temperature, 12 h; (D) Reagents and conditions: (a) (1) 1,4-diazabicyclo[2,2,2]-octane, CS₂, rt, 12 h, (2) BTC, reflux, 2 h (for two steps); (b) C₂H₅OH, room temperature, 12–24 h.

with CypA and protect the monkey cells against virus infections,¹³ CsA (Cyclosporin A) at the concentration of 10 μM, as the negative control, showed less than 10% SIV inhibiting proportion. Therefore, the antiviral results led us to further understand the exact inhibition mechanism of the compounds.

To clear whether the compound really target to HIV-1 CA, we used a spectrophotometrically method that measured the sample turbidity variation which was caused by the capsid assemble procession.^{9,14} This assay was used to probe for potential inhibitory effects of the thiourea compounds in this study. As shown in Figure 2, dissolution of native HIV-1 CA into assembly buffer (50 mM phosphate buffer, 2.5 M NaCl, pH 8.0, 0.2% v/v DMSO) led to an increase in absorbance at an initial rate of 102.60 mOD/min. Tang

et al had demonstrated that CAP-1 and its analogues could bind with CA and affect the rate of assembly. We found that the initial assembly rate in the presence of CAP-1 decreased to 52.46 mOD/min. For the identification of new assembly inhibitors, we added our test compounds and expected to delay the initial rate of CA assembly.

The presence of compound **T1** could moderate decrease the assembly rate of CA to 91.03 mOD/min. The modification of 3-bromo phenyl could slightly influence the assembly rate which decrease to 88.09 mOD/min in the existence of **T2**. Interestingly, compared with **T2**, the elimination of the nitro-group in pyrimidine (**T3**) thoroughly loss the inhibition capability. Like CAP-1, the title compounds **D1–D27** could more or less decrease the

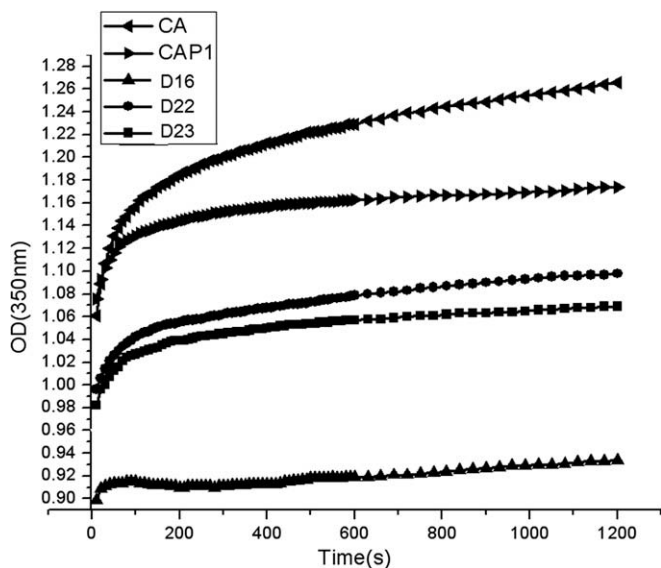


Figure 2. The effects of CA-binding compounds on in vitro CA assembly by the turbidity assay. Initial rate of the reaction: CA only (102.60 mOD/min); CAP-1 (52.46 mOD/min); **D16** (15.77 mOD/min); **D22** (31.20 mOD/min); **D23** (36.43 mOD/min); The reaction can be balance at the end of time.

assembly rate of CA in our study (Table 2 and Fig. 2). We then evaluated the influence of substituted phenyl group at Ar₁. As shown in Table 2, for *meta*-substituted derivatives, incorporation of an electron withdrawing group, for example, a chloride (**D16**, assembly rate = 15.77 mOD/min) resulted in a significant decrease of the CA assembly rate compared with none substituted phenyl compound (**D8**, assembly rate = 39.21 mOD/min). And, we investigated

Table 2
Assembly inhibitory data of thiourea derivatives

Entry	Assembly rate (mOD/min ^a)
T1	91.03
T2	88.09
T3	NA ^b
D1	66.65
D2	60.00
D3	69.60
D4	49.63
D5	49.20
D6	59.14
D7	67.80
D8	63.60
D9	64.64
D10	78.60
D11	55.71
D12	65.69
D13	19.57
D14	73.80
D15	76.20
D16	15.77
D17	29.00
D18	40.01
D19	64.80
D20	45.89
D21	39.21
D22	31.20
D23	36.43
D24	26.30
D25	27.38
D26	52.50
D27	58.97

^a mOD, millioptical density units.

^b NA, no activity.

the influence of the Ar₂ group in the inhibitory potency of HIV-1 CA assembly. Compared **D1** (assembly rate = 66.65 mOD/min) with **D6** (assembly rate = 59.14 mOD/min), it was found that introduction of naphthalene ring resulted in a slight loss of activity. The assembly rate of CA in the presence of compound **D24** (assembly rate = 26.30 mOD/min) with 4-methoxybenzene group was approximate to the presence of compound **D17** (assembly rate = 29.00 mOD/min) with a methoxazole group. Substitutions with thiazole group conducted to attenuated activity. For example, compared with the influences of **D17** and **D20**, the assembly rates in the presence of **D26** and **D27** increased to 52.50 mOD/min and 58.97 mOD/min, respectively. The introduction of isobenzofuran-1(3*H*)-one group (**D13**, assembly rate = 19.57 mOD/min) could significantly improve the inhibition of CA assembly when contrasted with initial 3-nitro-4-methyl phenyl group (**D2**, assembly rate = 60.00 mOD/min).

As seen in Table 3, the dose ratio of test compounds and CA increased sequentially as 0.5:1, 1:1, and 2:1, and the results revealed that the assembly effect also correspondingly amplified, which demonstrated that the assembly rate was changed in a dose-dependent manner. These results indicated that these CA-binding compounds could inhibit capsid assembly in vitro in a dose-dependent manner.

It has been demonstrated that CypA efficiently catalyzed the *cis*/*trans* isomerization of Gly-Pro within the isolated NTD of HIV-1 CA.¹⁵ And, CypA could also function by weakening the association between CA strips, thereby promoting disassembly of the viral core. Thus, the compound that can bind to CypA and inhibit its PPIase activity could be a potent inhibitor of HIV-1 replication. With the quick developments^{11,12,16} of CypA inhibitors, new discoveries made by Jean-Francois¹¹ indicated that the substituted phenyl can insert into the pocket A of CypA. Li¹² et al. also reported that sulfa-methoxazole group was an effective segment which could insert into the saddle pocket B of CypA. Since our compounds had similar active segments as those found by Jean-Francois and Li, we subsequently evaluated their binding activities with CypA and their PPIase inhibitory activities.

It had been reported that the tryptophan residue (Trp121) around the CypA binding site could be used as an intrinsic probe for studying the interaction between CypA and its ligand.¹⁷ The indole side chain of Trp121 can be validated as a major determinant in immunosuppressant drug recognition and the separation of PPIase catalytic efficiency from CysA affinity by the complementary gain and loss of CysA sensitivity to mutation to or from tryptophan. Therefore, we investigated the binding affinity of thiourea compounds against CypA by using the published intrinsic fluorescence titration technique.¹⁸ The inhibitory activity of the compounds on PPIase could be determined by a standard spectrophotometric method¹⁹, in which the rate constants for the *cis*-*trans* conversion were evaluated by fitting the data to the integrated first-order rate equation through nonlinear least-square analysis. As the positive control, CysA showed a concentration for 50% of the maximum inhibitory (IC₅₀) value of 9 nM against the PPIase activity of CypA. Our results indicated that except **T3**, all the thiourea compounds could bind to CypA with binding affinities (K_d values) ranging from 51.0 μM to 512.8 μM (Table 4). Among them, 15 compounds exhib-

Table 3
The CA assembly effect of different ratio compound:CA

D16 ratio Compound:CA	Assembly rate (mOD ^a /min)	D17 ratio Compound:CA	Assembly rate (mOD/min)
0.5:1	43.20	0.5:1	52.20
1:1	38.40	1:1	42.00
2:1	11.40	2:1	19.37

^a mOD, millioptical density units.

Table 4

Equilibrium affinity constants and in vivo IC₅₀ values for interaction of thiourea derivatives with CypA

Entry	K _d ^a (μM)	PPlase activity IC ₅₀ ^b (μM)	Entry	K _d (μM)	PPlase activity IC ₅₀ (μM)
T1	73.3	0.74	D13	96.6	0.59
T2	79.3	0.81	D14	109.5	0.35
T3	200.5	NA ^c	D15	128.5	0.38
D1	124.4	NA	D16	79.6	0.33
D2	88.9	0.46	D17	107.3	0.69
D3	125.1	NA	D18	100.7	NA
D4	222.2	NA	D19	116.5	0.60
D5	133.3	NA	D20	118.8	NA
D6	171.8	NA	D21	88.1	0.58
D7	147.1	NA	D22	88.6	0.45
D8	512.8	NA	D23	55.8	0.65
D9	141.0	NA	D24	60.8	NA
D10	140.4	NA	D25	51.6	0.16
D11	227.3	NA	D26	51.0	0.13
D12	NA	NA	D27	76.9	0.45

^a K_d values were determined from intrinsic tryptophan fluorescence titration assays at 25 °C.

^b PPlase IC₅₀ values were determined from enzyme inhibition assays at 6 °C.

^c NA, no activity.

ited potent PPlase inhibitory activities (IC₅₀ < 1 μM). These results suggested that the thiourea compounds might disrupt the disassembly process of the HIV-1 CA complexes by inhibiting CypA's activity to catalyze the cis/trans-isomerization of Gly89-Pro90 peptide bond of HIV-1 CA.

The further evaluation of the CypA PPlase inhibitory activities of the thiourea compounds showed that the substitution at Ar₁ group could significantly affect the inhibitory effect. The introduction of chlorine atom in *m*-position phenyl resulted in a very active compound **D16** (K_d = 79.6 μM, IC₅₀ = 0.33 μM). However, shifting the chloride atom from *meta* (**D16**) to *para* position (**D17**, K_d = 107.3 μM, IC₅₀ = 0.69 μM), could obviously decrease the binding affinities, and attenuate the inhibitory activities correspondingly (IC₅₀ value: **D17** > **D16**). In addition, the compounds with methyl group (**D20**, K_d = 118.8 μM) or methoxyl group (**D18**,

K_d = 100.7 μM) in *para*-phenyl only displayed very weak binding affinities but no inhibitory activities.

Regarding the influence of the substitution at Ar₂, except **D2** and **D13**, compounds **D1–D13** showed no PPlase inhibiting activities, indicating that naphthalene and isobenzofuran-1(3*H*)-one group substituted for Ar₂ did not contribute to the inhibition of PPlase activity. Compared with isobenzofuran-1(3*H*)-one of **D5**, the larger sulfonamide group of **D18** can contribute to the amelioration of PPlase inhibition. Remarkably, the introduction of sulfathiazole group (**D26**, K_d = 51.0 μM, IC₅₀ = 0.13 μM) showed the best enzymatic inhibitory activity among the Ar₂ groups.

Fifteen compounds in our study were found to inhibit both the CA assembly and CypA PPlase activities. We also performed the HIV-1 protease²⁰ and integrase^{21,22} inhibitory assays with the thiourea compounds to check if they can interact with another two critical proteins: HIV-1 protease and integrase. The results showed that these compounds did not inhibit the activity of HIV-1 protease since none of their final UV absorptions decreased more than 5%, and all the compounds tested showed lower than 20% of inhibition of HIV-1 integrase activities at 20 μM concentration. Our results indicated that the thiourea compounds did not inhibit the activities of HIV-1 protease and integrase. The antiviral activity of the compounds in our study might be due to the specific inhibition of HIV-1 CA and CypA.

To understand the molecular mechanism of the inhibitors, we carried out molecular docking analysis using the program AUTODOCK.²³ The docking results revealed that the thiourea derivatives inserted into the hydrophobic cavity of HIV-1 CA and the saddle pockets of CypA. As shown in Figure 3A, the docking pose of **D23** represented one of the binding models of the inhibitors and HIV-1 CA. The 3-chloro-4-methoxyl-phenyl group of compound **D23** inserted into the hydrophobic cavity, which composed by residues Val 27, Ala31, His62, Ala65, Leu138 and Leu141. The binding model indicated that the chlorine or bromine in *meta*-position of Ar₁ could contribute to the strong hydrophobic interaction between the small inhibitor and the hydrophobic cavity. Both the docking analysis data and the above experimental results revealed that the thiourea compounds with chlorine or bromine in *meta*-position of Ar₁ were potent assembly inhibitors of HIV-1 CA.

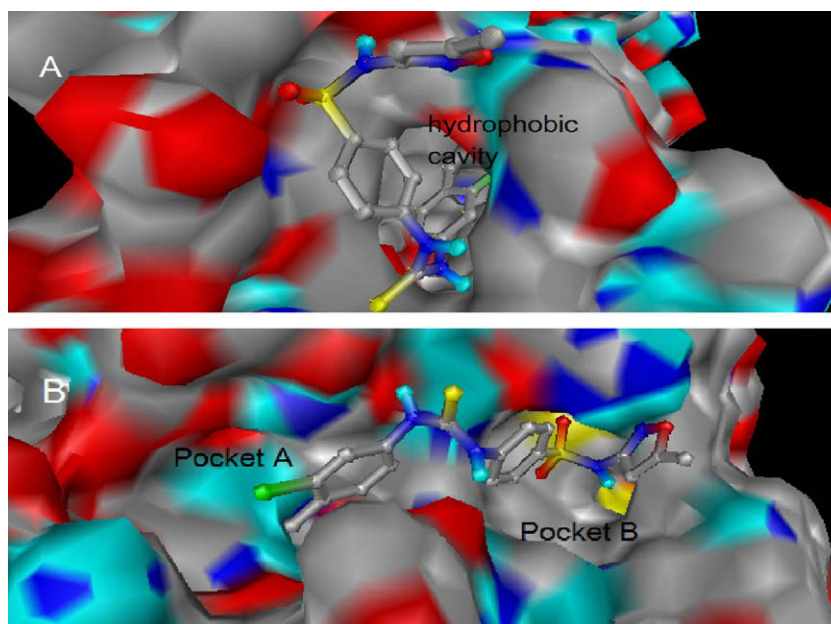


Figure 3. The molecular models of **D23** bind with CA NTD and CypA. (A) The molecular model of **D23** binds with CA NTD. The substituted phenyl of **D23** inserted into the hydrophobic cavity; the sulfamethoxazole group exposed to the surface of HIV-1 CA. (B) The molecular model of **D23** binds with CypA. The small molecule inserted into the saddle pockets (pocket A and pocket B); the figures were produced by Pmv.

Subsequently, we analyzed the interaction of the Ar₂ group of the thiourea compounds with HIV-1 CA. The oxygen of isoxazole of compound **D23** formed a hydrogen bond with the backbone hydrogen of Gly61, while another hydrogen bond was formed between the hydrogen of sulfamide and the oxygen of Thr58. The two hydrogen bonds may facilitate the binding affinity between the inhibitor and HIV-1 CA protein. Moreover, we studied the interaction between other substitutions of Ar₂ and HIV-1 CA. Interestingly, for the compound **D25**, the backbone hydrogen of Gly61 could also form hydrogen bonds with the nitrogen of thiazole. Remarkably, all the sulfamide groups could form a hydrogen bond with HIV-1 CA. Therefore, in the presence of the same Ar₁, the differences of inhibitory activities relied on the number of hydrogen bonds between the Ar₂ group and HIV-1 CA. These data indicated that the most effective assembly inhibitors of HIV-1 CA must be the compounds that contained chloride substitution in *meta*-phenyl of Ar₁ group, and their Ar₂ group should have strong interaction with HIV-1 CA protein.

We also performed docking analysis for the compounds that bound to CypA (Fig. 3B). As a typical example, the compound **D23** inserted into the active saddle grooves of CypA. The 3-chloro-4-methoxyl-phenyl of **D23** directed toward the pocket A composed of residues Gly72, Ser110, Gln111 and Lys82. The 3-chloro-4-methoxyl-phenyl could occupy more suitable space of pocket A, and contribute to the strong binding affinity. In addition, additional van der Waals was developed between the 3-chloride atom of **D23** and the side chain of Lys82. Meanwhile, the sulfamethoxazole group of **D23** could insert into the pocket B which consisted of Arg55, Phe60, Ala101, Ala103, Phe113, Leu122, and His126. The sulfamethoxazole group could provide two aryl rings for hydrophobic interaction with CypA. The oxygen of isoxazole could form hydrogen bonds with the guanidyl hydrogen atoms of Arg55. As an active pocket, the pocket B needs more hydrogen bonds to enhance the binding affinity. Consequently, the Ar₂ which had more hydrogen receptors and donors would facilitate the binding. In this study, sulfathiazole and sulfamethoxazole substitutions could give sulfamide group which contains hydrogen and oxygen as the hydrogen donor and receptor. Furthermore, thiazole and isoxazole also had some hetero-atoms as good hydrogen receptors. Therefore, it is clear that the introduction of sulfathiazole and sulfamethoxazole group could improve the binding affinity. Based on these analyses, we could say that the compounds composed of the chloride substitution in *meta*-position phenyl at Ar₁ and sulfamethoxazole group at Ar₂ might display distinguished binding activity with CypA.

According to molecular docking analyses, the binding models of the dual inhibitors should contain one fragment as suitable substituted phenyl, such as chloride atom substitution in *meta*-phenyl to

insert into both the cavity of HIV-1 CA and pocket A of CypA, and another segment such as sulfamethoxazole or sulfthiazole to form hydrogen bonds and hydrophobic interactions with HIV-1 CA and CypA. The inhibitory data of our dual inhibitors were summarized in Table 5.

3. Conclusion

In this study, we synthesized a series of thiourea derivatives targeting both HIV-1 CA and CypA to disrupt the processes of the assembly and uncoating of HIV-1 CA. The biological experiment results confirmed that 15 compounds could block HIV-1 replication by binding to CypA to inhibit its PPlase activity and uncoating, and by inserting into HIV-1 CA to disrupt its assembly. In addition, molecular docking analyses were also used to elucidate the binding models of the inhibitors to the two targets, HIV-1 CA and CypA. The compounds consisted of Ar₁ with chloride substitution in *meta*-position phenyl and Ar₂ with sulfamethoxazole group displayed potent assembly inhibitory activities, CypA binding affinities, the PPlase inhibitory activities and antiviral activities. The further characterizations of these compounds in vivo are on-going.

4. Experimental

4.1. Chemistry

All materials were commercially available and used without further purification. All the titled compounds were characterized by ¹H NMR spectra on a Varian 300 MHz or Bruke AM-300 spectrometer using the solvents described. Chemical shifts were reported in δ ppm (parts per million) relative to tetramethyl silane (TMS) except for deuterated water (D₂O) and the signals were quoted as s (singlet), d (doublet), t (triplet), q (quartet), and m (multiplet). The mass spectra (EI or ESI) were recorded. Melting points were determined on a XA-4 instrument which was uncorrected.

4.2. General synthetic procedures

As shown in Scheme 1, the compounds could be prepared by different types of amines and corresponding isothiocyanates. Scheme 1A outlined the preparation of the thiourea derivatives of **T1–T3**. The route includes three steps: First, the preparation of corresponding phenyl isothiocyanates. In the presence of 1,4-diazabicyclo[2,2,2]-octane, salts of dithiocarbamic acid were prepared by reacting arylamines with carbon disulfide, followed by subsequent conversion to aromatic isothiocyanates by reacting with bis(trichloromethyl)carbonate (BTC). And the phenyl isothiocyanates were isolated by column chromatography or vacuum distillation. Second, the preparation of *N*⁴-(2-aminoethyl)-*N*²,*N*²-diethyl-6-methyl-5-nitropyrimidine-2,4-diamine and *N*⁴-(2-aminoethyl)-*N*²,*N*²-diethyl-6-methylpyrimidine-2,4-diamine. 4-Chloro-*N,N*-diethyl-6-methyl-5-nitropyrimidin-2-amine was synthesized as Scheme 1A described, and compounds was prepared from it by amination. 4-Chloro-*N,N*-diethyl-6-methylpyrimidin-2-amine was synthesized by 2-(diethylamino)-6-methylpyrimidin-4-ol reacting with POCl₃. *N*⁴-(2-Aminoethyl)-*N*²,*N*²-diethyl-6-methylpyrimidine-2,4-diamine was synthesized from 4-chloro-*N,N*-diethyl-6-methylpyrimidin-2-amine and 1,2-diaminoethane in the presence of Na₂CO₃. Finally, title compounds **T1–T3** were synthesized from *N*⁴-(2-aminoethyl)-*N*²,*N*²-diethyl-6-methyl-5-nitropyrimidine-2,4-diamine or *N*⁴-(2-aminoethyl)-*N*²,*N*²-diethyl-6-methylpyrimidine-2,4-diamine corresponding phenyl isothiocyanates in the presence of triethylamine. Scheme 1B–D outlined the preparation of the thiourea derivatives of **D1–D27**. As shown

Table 5
The list of dual inhibitors and their inhibitory data

Entry	Capsid assembly rate (mOD/min)	Cyclophilin A PPlase IC ₅₀ (μM)
T1	91.03	0.74
T2	88.09	0.81
D2	60.00	0.46
D13	19.57	0.59
D14	73.80	0.35
D15	76.20	0.38
D16	15.77	0.33
D17	29.00	0.69
D19	64.80	0.60
D21	39.21	0.58
D22	31.20	0.45
D23	36.43	0.65
D25	27.38	0.16
D26	52.50	0.13
D27	58.97	0.45

in Scheme 1C, isobenzofuran-1(3H)-one was prepared by the reaction between isobenzofuran-1,3-dione and NaBH₄ in THF.²⁵ We used potassium nitrate in sulfuric acid to get the 6-nitrophthalide smoothly as described in the literature.²⁶ Then, 6-nitrophthalide was reduced by stannous chloride in hydrochloric acid to 6-aminophthalide. Naphthylamine and sulfonamide derivatives could be gotten from commercial Company (Alfa). The thiourea derivatives were synthesized from aromatic isothiocyanate (the same preparation as Scheme 1A) and substituted aromatic amino. All the title compounds **D1–D27** were recrystallized in methanol. The structures of these compounds were confirmed by ESI-MS/EI-MS and ¹H NMR. The purities of these compounds were identified by HPLC.

4.2.1. 1-(3-Chloro-4-methylphenyl)-3-(2-(2-(diethylamino)-6-methyl-5-nitropyrimidin-4-ylamino)ethyl)thiourea (T1)

A mixture of compound 3-chloro-4-methylphenyl isothiocyanate (0.183 g; 1 mmol) and N⁴-(2-aminoethyl)-N²,N²-diethyl-6-methyl-5-nitropyrimidine-2,4-diamine (0.27 g; 1 mmol) was stirred in acetone. Then, N(C₂H₅)₃ (0.02 g, 0.1 mmol) was added into the mixture. After reflux stirring 5 h, the mixture was concentrated under reduced pressure then purified by column chromatography (silica gel, dichloromethane/methanol = 4:1, v/v). Compound **T1** was obtained as yellow solid, mp 178 °C, yield = 64.9%.

¹H NMR (300 MHz, CDCl₃) δ 1.13–1.20 (m, 6H), 2.33 (s, 3H), 2.72 (s, 3H), 3.45–3.53 (m, 2H), 3.64–3.68 (m, 2H), 3.85–3.90 (m, 4H), 6.52 (s, 1H), 6.91–6.95 (m, 1H), 7.11–7.15 (m, 2H), 7.58 (s, 1H), 8.83 (s, 1H); ESI-MS: *m/z* = 452.15 (M+H⁺); RP-HPLC: *t*_R = 4.4 min (10% water in menthol), purity > 94%.

4.2.2. 1-(3-Bromophenyl)-3-(2-(2-(diethylamino)-6-methyl-5-nitropyrimidin-4-ylamino)ethyl)thiourea (T2)

Compound **T2** was prepared in the same way as **T1**, yellow needle solid, mp 144–146 °C, yield = 63.6%. ¹H NMR (300 MHz, CDCl₃) δ 1.13–1.20 (m, 6H), 2.70 (s, 3H), 3.44–3.51 (m, 2H), 3.62–3.70 (m, 2H), 3.85–3.91 (m, 4H), 6.53 (s, 1H), 7.05–7.380 (m, 4H), 7.57 (s, 1H), 8.84 (s, 1H); ESI-MS: *m/z* = 482.10, 484.09 (M+H⁺). RP-HPLC: *t*_R = 6.3 min (10% water in menthol), purity > 96%.

4.2.3. 1-(3-Bromophenyl)-3-(2-(2-(diethylamino)-6-methylpyrimidin-4-ylamino)ethyl)thiourea (T3)

Compound **T3** was prepared in the same way as **T1**, yellow needle solid, mp 117–118 °C yield = 63.6%. ¹H NMR (300 MHz, CDCl₃) δ 1.21 (s, 6H), 2.38 (s, 3H), 3.56–3.94 (m, 8H), 5.83 (s, 1H), 7.15–7.720 (m, 4H), 8.20 (s, 1H), 9.57 (s, 1H), 11.11 (s, 1H); ESI-MS: *m/z* = 437.11 (M+H⁺); RP-HPLC: *t*_R = 3.8 min (10% water in menthol), purity > 99%.

4.2.4. 1-(4-Methoxyphenyl)-3-(naphthalen-2-yl)thiourea (D1)

A mixture of compound 4-methoxyphenyl isothiocyanate (0.167 g; 1 mmol) and naphthalen-2-amine (0.14 g; 1 mmol) was stirred in ethanol. After stirring overnight, the mixture was filtered. The precipitation was recrystallized in methanol. Compound **D1** was obtained as white solid, mp 179–180 °C, yield = 64.9%. Compound **D1**: ¹H NMR (300 MHz, DMSO-*d*₆) δ 3.75 (s, 3H), 6.91–6.93 (d, *J* = 6.0 Hz, 2H), 7.34–7.36 (d, *J* = 6.0 Hz, 2H), 7.46–7.51 (m, 2H), 7.59–7.62 (d, 2H), 7.83–7.87 (t, 3H), 7.98 (s, 1H), 9.73–9.86 (d, 2H), EI-MS: *m/z* = 308. RP-HPLC: *t*_R = 4.4 min (10% water in menthol), purity > 97%.

4.2.5. 1-(3-Chloro-4-methylphenyl)-3-(4-methyl-3-nitrophenyl)thiourea (D2)

Compound **D2** was prepared in the same way as **D1**, yellow solid, mp 186–187 °C, yield = 85.4%. ¹H NMR (300 MHz, DMSO-*d*₆) δ 2.28 (s, 3H), 7.27–7.30 (dd, 2H), 7.42–7.45 (d, 1H), 7.58 (s, 1H), 7.66 (d, *J* = 2.4 Hz, 1H), 8.22 (d, *J* = 2.4 Hz, 1H); EI-MS: *m/z* = 335. RP-HPLC: *t*_R = 4.4 min (10% water in menthol), purity > 97%.

4.2.6. 1-(3-Bromophenyl)-3-(3-oxo-1,3-dihydroisobenzofuran-5-yl)thiourea (D3)

Compound **D3** was prepared in the same way as **D1**, white solid, mp 166–168 °C, yield = 76.3%. ¹H NMR (300 MHz, DMSO-*d*₆) δ 5.38 (s, 2H), 7.29–7.32 (t, 2H), 7.40–7.42 (m, 1H), 7.60–7.64 (d, 1H), 7.76 (d, *J* = 3 Hz, 1H), 7.81–7.79 (t, 1H), 7.98 (t, *J* = 3 Hz, 1H); EI-MS: *m/z* = 362, 364. RP-HPLC: *t*_R = 3.3 min (10% water in menthol), purity > 98%. RP-HPLC: *t*_R = 3.3 min (10% water in menthol), purity > 98%.

4.2.7. 1-(4-Chlorophenyl)-3-(3-oxo-1,3-dihydroisobenzofuran-5-yl)thiourea (D4)

Compound **D4** was prepared in the same way as **D1**, white solid, mp 201–202 °C, yield = 78.5%. ¹H NMR (300 MHz, DMSO-*d*₆) δ 5.41 (s, 2H), 7.40–7.66 (dd, 4H), 7.80–7.83 (dd, 2H), 8.02 (s, 1H), 10.09–10.10 (d, 2H); EI-MS: *m/z* = 318. RP-HPLC: *t*_R = 3.3 min (10% water in menthol), purity > 98%.

4.2.8. 1-(3-Chlorophenyl)-3-(3-oxo-1,3-dihydroisobenzofuran-5-yl)thiourea (D5)

Compound **D5** was prepared in the same way as **D1**, white solid, mp 175–176 °C, yield = 73.2%. ¹H NMR (300 MHz, DMSO-*d*₆) δ 5.40 (s, 2H), 7.18–7.32 (m, 1H), 7.36–7.39 (m, 2H), 7.61–7.68 (t, 2H), 7.78–7.83 (m, 1H), 8.06 (s, 1H), 10.12–10.19 (d, 2H); EI-MS: *m/z* = 318. RP-HPLC: *t*_R = 3.3 min (10% water in menthol), purity > 99%.

4.2.9. 1-(4-Methoxyphenyl)-3-(3-oxo-1,3-dihydroisobenzofuran-5-yl)thiourea (D6)

Compound **D6** was prepared in the same way as **D1**, white solid, mp 183–184 °C, yield = 74.5%. Compound **D6**: ¹H NMR (300 MHz, DMSO-*d*₆) δ 3.74 (s, 3H), 5.38 (s, 2H), 6.90–7.35 (dd, 4H), 7.58 (d, *J* = 12 Hz, 1H), 7.77 (d, *J* = 12 Hz, 1H), 8.01 (s, 1H), 9.84–9.87 (d, 2H); EI-MS: *m/z* = 314. RP-HPLC: *t*_R = 2.9 min (10% water in menthol), purity > 99%.

4.2.10. 1-(2,4,5-Trichlorophenyl)-3-(3-oxo-1,3-dihydroisobenzofuran-5-yl)thiourea (D7)

Compound **D7** was prepared in the same way as **D1**, white solid, mp 185–186 °C, yield = 81.2%. ¹H NMR (300 MHz, DMSO-*d*₆) δ 5.41 (s, 2H), 7.64–7.80 (dd, 2H), 7.82–7.97 (s, 2H), 8.06 (s, 1H), 9.80 (s, 1H), 10.36 (s, 1H); ESI-MS: *m/z* = 386.2 (M+H⁺). RP-HPLC: *t*_R = 4.3 min (10% water in menthol), purity > 99%.

4.2.11. 1-(3,5-Difluorophenyl)-3-(3-oxo-1,3-dihydroisobenzofuran-5-yl)thiourea (D8)

Compound **D8** was prepared in the same way as **D1**, white solid, mp 190–191 °C, yield = 69.1%. ¹H NMR (300 MHz, DMSO-*d*₆) δ 5.40 (s, 2H), 7.07–7.14 (t, 1H), 7.31–7.50 (t, 1H), 7.52–7.77 (m, 1H), 7.79–8.03 (dd, 2H), 9.65 (s, 1H), 10.17 (s, 1H); ESI-MS: *m/z* = 321.1 (M+H⁺). RP-HPLC: *t*_R = 2.9 min (10% water in menthol), purity > 99%.

4.2.12. 1-(3-Oxo-1,3-dihydroisobenzofuran-5-yl)-3-*m*-tolylthiourea (D9)

Compound **D9** was prepared in the same way as **D1**, white solid, mp 183–185 °C, yield = 78.2%. ¹H NMR (300 MHz, DMSO-*d*₆) δ 2.28 (s, 3H), 5.37 (s, 2H), 6.90–7.35 (dd, 4H), 7.58–7.82 (dd, 2H), 8.01 (s, 1H), 9.98 (s, 2H); EI-MS: *m/z* = 298. RP-HPLC: *t*_R = 3.1 min (10% water in menthol), purity > 99%.

4.2.13. 1-(3-Fluorophenyl)-3-(3-oxo-1,3-dihydroisobenzofuran-5-yl)thiourea (D10)

Compound **D10** was prepared in the same way as **D1**, white solid, mp 190–191 °C, yield = 72.3%. ¹H NMR (300 MHz, DMSO-*d*₆) δ 5.39 (s, 2H), 7.13 (t, *J* = 2.4 Hz, 1H), 7.33–7.38 (t, 2H), 7.47–7.49

(d, 1H), 7.61–7.66 (t, 1H), 7.79 (m, $J = 2.4$ Hz, 1H), 8.03 (s, 1H), 9.99–10.01 (d, 2H); ESI-HRMS: $m/z = 303.05980$ ($M+H^+$, calcd for $C_{15}H_{11}N_2O_2S_1F_1$, 303.05253). RP-HPLC: $t_R = 3.1$ min (10% water in menthol), purity > 99%.

4.2.14. 1-(4-Fluorophenyl)-3-(3-oxo-1,3-dihydroisobenzofuran-5-yl)thiourea (D11)

Compound **D11** was prepared in the same way as **D1**, white solid, mp 174–175 °C, yield = 70.6%. 1H NMR (300 MHz, DMSO- d_6) δ 5.40 (s, 2H), 7.16–7.22 (t, 2H), 7.46–7.50 (t, 2H), 7.61 (d, $J = 8.1$ Hz, 1H), 7.79–7.82 (d, $J = 8.1$ Hz, 1H), 8.012 (s, 1H), 9.95–10.01 (d, 2H); ESI-MS: $m/z = 303.1$ ($M+H^+$). RP-HPLC: $t_R = 3.0$ min (10% water in menthol), purity > 97%.

4.2.15. 1-(3-Oxo-1,3-dihydroisobenzofuran-5-yl)-3-*o*-tolylthiourea (D12)

Compound **D12** was prepared in the same way as **D1**, white solid, mp 183–185 °C, yield = 78.2%. 1H NMR (300 MHz, DMSO- d_6) δ 2.26 (s, 3H), 5.35 (s, 2H), 6.95–7.00 (t, 1H), 7.14 (d, $J = 7.8$ Hz, 1H), 7.18 (d, $J = 7.8$ Hz, 1H), 7.57 (d, $J = 10$ Hz, 1H), 7.63 (d, $J = 10$ Hz, 1H), 7.79–7.82 (d, 1H), 8.02 (s, 1H), 8.12 (s, 1H), 9.36 (s, 1H); ESI-MS: $m/z = 299.1$ ($M+H^+$). RP-HPLC: $t_R = 3.3$ min (10% water in menthol), purity > 99%.

4.2.16. 1-(3-Chloro-4-methylphenyl)-3-(3-oxo-1,3-dihydroisobenzofuran-5-yl)thiourea (D13)

Compound **D13** was prepared in the same way as **D1**, white solid, mp 189–190 °C, yield = 75.1%. 1H NMR (300 MHz, DMSO- d_6) δ 2.28 (s, 3H), 5.38 (s, 2H), 7.29–7.30 (t, $J = 3$ Hz, 2H), 7.60–7.63 (d, 2H), 7.79–7.80 (d, $J = 3$ Hz, 1H), 7.79 (s, 1H); EI-MS: $m/z = 332$. RP-HPLC: $t_R = 4.4$ min (10% water in menthol), purity > 95%.

4.2.17. 4-(3-(4-Fluorophenyl)thioureido)-*N*-(5-methylisoxazol-3-yl)benzenesulfonamide (D14)

Compound **D14** was prepared in the same way as **D1**, white solid, mp 188–190 °C, yield = 77.2%. 1H NMR (300 MHz, DMSO- d_6) δ 2.29 (s, 3H), 6.16 (s, 1H), 7.16–7.22 (t, 2H), 7.44–7.49 (t, 2H), 7.71 (d, $J = 9$ Hz, 2H), 7.78 (d, $J = 9$ Hz, 2H), 10.11–10.18 (d, 2H), 11.41 (s, 1H); ESI-MS: $m/z = 407.1$ ($M+H^+$). RP-HPLC: $t_R = 10.6$ min (10% water in menthol), purity > 97%.

4.2.18. 4-(3-(3-Fluorophenyl)thioureido)-*N*-(5-methylisoxazol-3-yl)benzenesulfonamide (D15)

Compound **D15** was prepared in the same way as **D1**, white solid, mp 169–170 °C, yield = 81.3%. 1H NMR (300 MHz, DMSO- d_6) δ 2.29 (s, 3H), 6.16 (s, 1H), 7.13–7.18 (t, 1H), 7.35 (d, $J = 7.5$ Hz, 2H), 7.45–7.48 (d, $J = 7.5$ Hz, 2H), 7.72 (d, $J = 9$ Hz, 2H), 7.77 (d, $J = 9$ Hz, 2H), 10.15–10.17 (d, 2H), 11.39 (s, 1H); ESI-MS: $m/z = 407.1$ ($M+H^+$). RP-HPLC: $t_R = 6.9$ min (10% water in menthol), purity > 98%.

4.2.19. 4-(3-(3-Chlorophenyl)thioureido)-*N*-(5-methylisoxazol-3-yl)benzenesulfonamide (D16)

Compound **D16** was prepared in the same way as **D1**, white solid, mp 179–180 °C, yield = 83.7%. 1H NMR (300 MHz, DMSO- d_6) δ 2.28 (s, 3H), 6.16 (s, 1H), 7.19–7.22 (m, 2H), 7.37–7.42 (m, 2H), 7.67–7.82 (m, 5H), 10.25–10.31 (d, 2H), 11.41 (s, 1H); ESI-MS: $m/z = 423.0$ ($M+H^+$). RP-HPLC: $t_R = 10.4$ min (10% water in menthol), purity > 99%.

4.2.20. 4-(3-(4-Chlorophenyl)thioureido)-*N*-(5-methylisoxazol-3-yl)benzenesulfonamide (D17)

Compound **D17** was prepared in the same way as **D1**, white solid, mp 177–178 °C, yield = 77.9%. 1H NMR (300 MHz, DMSO- d_6) δ 2.29 (s, 3H), 6.16 (s, 1H), 7.37 (d, $J = 10.5$ Hz, 2H), 7.48 (d,

$J = 10.5$ Hz, 2H), 7.65–7.82 (dd, 4H), 10.20–10.23 (d, 2H), 11.40 (s, 1H); ESI-MS: $m/z = 423.03469$ ($M+H^+$, calcd for $C_{17}H_{15}N_4O_3S_2Cl_1$, 423.02741). RP-HPLC: $t_R = 10.9$ min (10% water in menthol), purity > 99%.

4.2.21. 4-(3-(4-Methoxyphenyl)thioureido)-*N*-(5-methylisoxazol-3-yl)benzenesulfonamide (D18)

Compound **D18** was prepared in the same way as **D1**, white solid, mp 180–181 °C, yield = 80.4%. 1H NMR (300 MHz, DMSO- d_6) δ 2.30 (s, 3H), 3.78 (s, 3H), 6.15 (s, 1H), 6.90 (d, $J = 8.7$ Hz, 2H), 7.31 (d, $J = 8.7$ Hz, 2H), 7.72 (d, $J = 8.7$ Hz, 2H), 7.75 (d, $J = 8.7$ Hz, 2H), 9.97–10.01 (d, 2H), 11.37 (s, 1H); EI-MS: $m/z = 418$. RP-HPLC: $t_R = 9.0$ min (10% water in menthol), purity > 97%.

4.2.22. *N*-(5-Methylisoxazol-3-yl)-4-(3-*o*-tolylthioureido)benzenesulfonamide (D19)

Compound **D19** was prepared in the same way as **D1**, white solid, mp 187–188 °C, yield = 78.2%. 1H NMR (300 MHz, DMSO- d_6) δ 2.23 (s, 3H), 2.30 (s, 3H), 6.14 (s, 1H), 7.18 (d, $J = 8.7$ Hz, 2H), 7.22 (d, $J = 8.7$ Hz, 2H), 7.78 (m, 4H), 9.67 (s, 1H), 10.05 (s, 1H), 11.36 (s, 1H); ESI-MS: $m/z = 403.1$ ($M+H^+$). RP-HPLC: $t_R = 9.4$ min (10% water in menthol), purity > 98%.

4.2.23. *N*-(5-Methylisoxazol-3-yl)-4-(3-*p*-tolylthioureido)benzenesulfonamide (D20)

Compound **D20** was prepared in the same way as **D1**, white solid, mp 195–196 °C, yield = 69.2%. 1H NMR (300 MHz, DMSO- d_6) δ 2.28–2.30 (d, 6H), 6.15 (s, 1H), 7.14–7.34 (dd, 4H), 7.72–7.79 (m, 4H), 10.04–10.06 (d, 2H), 11.36 (s, 1H); ESI-MS: $m/z = 403.1$ ($M+H^+$). RP-HPLC: $t_R = 9.7$ min (10% water in menthol), purity > 97%.

4.2.24. *N*-(5-Methylisoxazol-3-yl)-4-(3-phenylthioureido)benzenesulfonamide (D21)

Compound **D21** was prepared in the same way as **D1**, white solid, mp 166–167 °C, yield = 68.1%. 1H NMR (300 MHz, DMSO- d_6) δ 2.30 (s, 3H), 6.15 (s, 1H), 7.15–7.18 (m, 1H), 7.35 (d, $J = 11.8$ Hz, 2H), 7.46 (d, $J = 11.8$ Hz, 2H), 7.78–7.79 (dd, 4H), 10.14–10.16 (d, 2H), 11.39 (s, 1H); EI-MS: $m/z = 388$. RP-HPLC: $t_R = 10.1$ min (10% water in menthol), purity > 99%.

4.2.25. 4-(3-(3-Bromophenyl)thioureido)-*N*-(5-methylisoxazol-3-yl)benzenesulfonamide (D22)

Compound **D22** was prepared in the same way as **D1**, white solid, mp 165–166 °C, yield = 69.8%. 1H NMR (300 MHz, DMSO- d_6) δ 2.29 (s, 3H), 6.16 (s, 1H), 7.27–7.36 (m, 2H), 7.42–7.45 (m, 1H), 7.45–7.82 (m, 5H), 10.23–10.31 (d, 2H), 11.41 (s, 1H); ESI-MS: $m/z = 467.0$, 469.0 ($M+H^+$). RP-HPLC: $t_R = 10.4$ min (10% water in menthol), purity > 95%.

4.2.26. 4-(3-(3-Chloro-4-methylphenyl)thioureido)-*N*-(5-methylisoxazol-3-yl)benzenesulfonamide (D23)

Compound **D23** was prepared in the same way as **D1**, white solid, mp 172–173 °C, yield = 81.2%. 1H NMR (300 MHz, DMSO- d_6) δ 2.30–2.33 (d, 6H), 6.16 (s, 1H), 7.30–7.33 (t, 2H), 7.62 (s, 1H), 7.71 (d, $J = 9$ Hz, 2H), 7.78 (d, $J = 9$ Hz, 2H), 10.15–10.22 (d, 2H), 11.39 (s, 1H); EI-MS: $m/z = 436$; RP-HPLC: $t_R = 12.1$ min (10% water in menthol), purity > 98%.

4.2.27. 4-(3-(4-Chlorophenyl)thioureido)-*N*-(4-methoxyphenyl)benzenesulfonamide (D24)

Compound **D24** was prepared in the same way as **D1**, white solid, mp 190–192 °C, yield = 68.2%. 1H NMR (300 MHz, DMSO- d_6) δ 3.67 (s, 3H), 6.79 (d, $J = 9$ Hz, 2H), 6.98 (d, $J = 9$ Hz, 2H), 7.38 (d, $J = 10$ Hz, 2H), 7.48 (d, $J = 10$ Hz, 2H), 7.60 (d, $J = 10$ Hz, 2H), 7.66 (d, $J = 10$ Hz, 2H), 9.87 (s, 1H), 10.13–10.16 (d, 2H); EI-MS:

$m/z = 436$. RP-HPLC: $t_R = 3.4$ min (10% water in menthol), purity > 99%.

4.2.28. 4-(3-(3-Chloro-4-methylphenyl)thioureido)-N-(thiazol-2-yl)benzenesulfonamide (D25)

Compound **D25** was prepared in the same way as **D1**, white solid, mp 190–192 °C, yield = 76.4%. ^1H NMR (300 MHz, DMSO- d_6) δ 2.30 (s, 3H), 6.82 (d, $J = 4.8$ Hz, 1H), 7.27 (d, $J = 4.8$ Hz, 1H), 7.38–7.66 (dd, 4H), 7.73–7.76 (dd, 4H), 10.04–10.15 (d, 2H), 12.70 (s, 1H); ESI-MS: $m/z = 439.0$ ($\text{M} + \text{H}^+$). RP-HPLC: $t_R = 7.2$ min (10% water in menthol), purity > 95%.

4.2.29. 4-(3-(4-Chlorophenyl)thioureido)-N-(thiazol-2-yl)benzenesulfonamide (D26)

Compound **D26** was prepared in the same way as **D1**, white solid, mp 199–200 °C, yield = 67.3%. ^1H NMR (300 MHz, DMSO- d_6) δ 6.82 (d, $J = 4.8$ Hz, 1H), 7.25 (d, $J = 4.8$ Hz, 1H), 7.38–7.53 (dd, 4H), 7.628–7.758 (d, 4H), 10.09–10.15 (d, 2H), 12.70 (s, 1H); ESI-MS: $m/z = 424.99620$ ($\text{M} + \text{H}^+$, calcd for $\text{C}_{16}\text{H}_{13}\text{N}_4\text{O}_2\text{S}_1\text{Cl}_1$, 424.98892). RP-HPLC: $t_R = 6.4$ min (10% water in menthol), purity > 95%.

4.2.30. N-(Thiazol-2-yl)-4-(3-*p*-tolylthioureido)benzenesulfonamide (D27)

Compound **D27** was prepared in the same way as **D1**, white solid, mp 196–197 °C, yield = 81.2%. ^1H NMR (300 MHz, DMSO- d_6) δ 2.28 (s, 3H), 6.82–6.83 (d, 1H), 7.13–7.16 (d, 2H), 7.24–7.26 (d, 2H), 7.31–7.34 (d, 2H), 7.63–7.74 (dd, 4H), 9.94–9.98 (d, 2H), 12.70 (s, 1H) ESI-MS: $m/z = 405.1$ ($\text{M} + \text{H}^+$). RP-HPLC: $t_R = 6.2$ min (10% water in menthol), purity = 95%.

4.3. Biological evaluation

4.3.1. Antiviral evaluation

Inhibition of SIV-induced syncytium in CEM174 cell cultures was measured in a 96-well microplate containing 2×10^5 CEM cells/ml infected with 100 TCID₅₀ of SIV per well and containing appropriate dilutions of the tested compounds. After 5 days of incubation at 37 °C in 5% CO₂ containing humidified air, CEM giant (syncytium) cell formation was examined microscopically. The EC₅₀ was defined as the compound concentration required to protect cells against the cytopathogenicity of SIV by 50%. AZT was used as the positive control at a concentration of 10 μM here. Its EC₅₀ is 0.0122 μM and TC₅₀ is above 100 μM in this system.

4.3.2. Assembly inhibitory assay

Ultraviolet spectrophotometry assay was performed at 350 nm on a WFZ800-D2 spectrophotometer. A 1.2 μl of concentrated ligand in DMSO (10 mM) was added to a 450 μl aqueous solution (2 ml of 5 M NaCl mixed with 1 ml of 200 mM NaH₂PO₄, pH 8.0), and 150 μl capsid protein (80 μM) was added to initiate the reaction. Spectral measurements were made every 10 s, following a short initial delay to allow sample equilibration. Relative assembly rates were estimated from initial slopes of the plots of absorbance versus time.

4.3.3. CypA/inhibitor binding affinity assay

Fluorescence measurements were performed on a SHIMADZU RF-5301PC fluorescence spectrophotometer. The experiments were carried out at room temperature in 20 mM Tris–HCl, 100 mM NaCl (pH 7.4) with the protein concentration set at 6 μM and the compound concentrations varied from 0 to 64 μM . The compounds were prepared in dimethylsulfoxide (DMSO) as a stock solution of 10 mM. The excitation wavelength was set at 280 nm, the emission range was from 300 nm to 380 nm, and the slit was set at 5 nm (EX) and 3 nm (EM). Fluorescence readings

were taken at the wavelength of maximum emission (340 nm). The fluorescence intensity versus the final compound concentration was integrated to the following equation, where F_0 stands for the initial fluorescence intensity of the protein solution without compound ($F_0/F = 1 + K_a \cdot C$). So the experimental data was analyzed of binding constants ($K_a = 1/K_d$).

4.3.4. CypA PPIase inhibitory assay

Suc-AAPF-pNA was dissolved in THF that contained LiCl (480 mM) to a concentration of 3 mM. Then, α -chymotrypsin was dissolved in 1 mM HCl to a concentration of 45 mg/ml. The assay buffer (93 μl of 50 mM HEPES, 100 mM NaCl; pH 8.0 at 0 °C) and CypA (2 μl of 6 μM stock solution) were pre-equilibrated for 3 h on ice. Immediately before the assay was started, 2 μl of α -chymotrypsin solution and 2 μl of peptide substrate were added to the assay mixture. After a delay from the onset of mixing (usually 6 s), absorbance value at the wavelength of 390 nm had been recorded on an Agilent 8453 spectrophotometer for 20 s. The progress curves were analyzed by fitting the data to the integrated first-order rate equation through nonlinear least-square analysis to evaluate the rate constants for the *cis*–*trans* conversion and the respective IC₅₀ was calculated with ORIGINPRO 7.5 software.

4.3.5. HIV-1 protease inhibitory assay

We tested the inhibition data for HIV-1 protease by ultraviolet spectrophotometry assay at 280 nm on a WFZ800-D2 spectrophotometer. The inhibitors (10 μM) were dissolved in 4.0 μl DMSO and incubated with HIV-1 protease (5 μM) in 200 μl assay buffer (0.1 M MES, 0.2 M NaCl, 5 mM EDTA, pH 5.5) at room temperature for 20 min. Then protease substrate (Lys-Ala-Arg-Val-Leu-Phe(NO₂)-Glu-Ala-Met, 100 μM) was added to initiate the reaction. The hydrolysis of the substrate was recorded as a linear decrease in UV absorbance at 280 nm over a 40-min time period. Inhibition ratio was determined from the A_i/A_0 , where A_i and A_0 were the absorption at 280 nm in the presence and absence of the inhibitor. Indinavir (10 μM) was used as positive control with final absorption decreased more than 90%.²⁰ Both **D5** and **D23** showed no inhibition of protease for their final absorptions decreased less than 5%.

4.3.6. HIV-1 integrase inhibitory assay

The recombinant HIV-1 integrase was purified from *Escherichia coli*. The oligonucleotides (d1, 5'-ACC CTT TTA GTC AGT GTG GAA AAT CTC TAC CAG T-3', d2, 5'-ACT GGT AGA GAT TTT CCA CAC TGA CTA AAA G-3', t1, 5'-TGA CCA AGG GCT AAT TCA CT-3' and t2, 5'-AGT GAA TTA GCC CTT GGT CA-3') were purchased from SBS Genetech Co., Ltd. The oligonucleotide d1 was synthesized to include a 5'-phosphorylated three base overhangs on the 5' end of the strand and the oligonucleotides t1 and t2 were biotinylated. The oligonucleotides d1 and d2 as well as t1 and t2 were mixed and boiled for 3 min. Then the mixture was cooled slowly and provided the donor substrate and the target substrate, respectively. The enzyme-linked immunosorbent assay was performed to detect the activity of integrase. The donor oligonucleotides were immobilized onto Covalink polystyrene microtiter plate (NUNC, Naperville, IL) under the catalysis of 0.05 M EDC (1-ethyl-3-(3-dimethylamino-propyl)-carbodiimide) in 100 μl 1-methylimidazole (10 mM pH 7) incubated at 50 °C for 5 h. Then the plates were washed with PBS buffer three times and stored with blocking buffer (PBS with 1% BSA and 0.2% sodium azide) at 4 °C over night. The coated plates were washed with PBS buffer three times and was added with 100 μl TM buffer per well (Tris–HCl 20 mM, pH 7.8, NaCl 25 mM, MgCl₂ 7.5 mM, β -mercaptoethanol 5 mM and BSA 50 $\mu\text{g}/\text{ml}$) containing the purified integrase with a final concentration of 0.05 mM. After incubation at 37 °C for 30 min, the target oligonucleotides (t1 and t2 mixture) were added and incubated for

1 h at 37 °C. After three washes with PBS containing 0.05% Tween 20 and two washes with PBS, the plates were blocked with 1% BSA at room temperature for 30 min. Then the integration products were detected and quantified using a pNPP Phosphatase Assay Kit (Biochain). The absorption at 405 nm was detected on Bio-Rad Model 550. For the inhibition assay, the integrase was incubated with 20 μ M compounds for 30 min before added to the reaction system and the following steps were the same as above. The inhibitory activity was determined by the decrease ratio of the final absorption. The Merck L-731988 was used as positive control.²⁷ The inhibitory ratio of compounds **D5** and **D23** were both below 20%.

4.4. Molecular modelling

The initial structures of our compounds were subjected to minimization using MOPAC in Chemoffice 2005 and the 3D structure of HIV-1 Capsid in complex with its inhibitor CAP-1 was recovered from the Protein Database (<http://www.rcsb.org>) with the code as 2JPR.¹⁰ Another 3D structure of CypA in complex with CsA was downloaded from Protein Database with the code 1CWA.²⁸ The advanced docking program AUTO-DOCK 4.0 was used to remove the small molecule and perform the automatic molecular docking with our compounds. The number of generations, energy evaluation, and docking runs were set to 370,000, 1,500,000, and 50, respectively, and the kinds of atomic charges were taken as Kollman-all-atom for macromolecular and Gasteiger-Hücel for the compounds. Molecular graphics images were produced using the UCSF Chimera package from the Resource for Biocomputing, Visualization, and Informatics at the University of California, San Francisco (supported by NIH P41 RR-01081).

Acknowledgments

This project was supported by the National Natural Science Foundation of China (No. 30670415). We thank Professor Fangqiu Li for her help in this work.

References and notes

- Coffin, J. M. *Science* **1995**, 267, 483.
- Rossmann, M. G. *Proc. Natl. Acad. Sci.* **1988**, 85, 4625.
- Popovic, M.; Tenner-Racz, K.; Pelsner, C.; Stellbrink, H.; Lunzen, J.; Lewis, G.; Kalyanaraman, V.; Gallo, C. R.; Racz, P. *Proc. Natl. Acad. Sci.* **2005**, 102, 14807.
- Stremlau, M. *Science* **2007**, 318, 1565.
- Ganser-Pornillos, B. K.; von Schwedler, U. K.; Stray, K. M.; Aiken, C.; Sundquist, W. I. *J. Virol.* **2004**, 78, 2545.
- Ganser-Pornillos, B. K.; Cheng, A.; Yeager, M. *Cell* **2007**, 131, 70.
- Sundquist, W. I.; Hill, P. C. *Cell* **2007**, 131, 17.
- Ternois, F.; Sticht, J.; Duquerroy, S.; Krausslich, H. G.; Rey, F. A. *Nat. Struct. Mol. Biol.* **2005**, 12, 678.
- Tang, C.; Loeliger, E.; Kinde, I.; Kyere, S.; Mayo, K.; Barklis, E.; Sun, Y.; Huang, M.; Summers, M. F. *J. Mol. Biol.* **2003**, 327, 1013.
- Kelly, B. N.; Kyere, S.; Kinde, I.; Tang, C.; Howard, R. B.; Robinson, H.; Sundquist, I. W.; Summers, F. M.; Hill, P. C. *J. Mol. Biol.* **2007**, 373, 355.
- Jean-Francois, G.; Julien, V.; Clément, M.; Guy, S.; Yea-Lih, L.; Alain, C. *J. Med. Chem.* **2006**, 49, 900.
- Li, J.; Chen, J.; Gui, C. S.; Li, Z.; Yu, Q.; Xu, Q.; Zhang, J.; Liu, H.; Xu, S.; Jiang, H. L. *Bioorg. Med. Chem.* **2006**, 14, 2209.
- Nisole, S.; Lynch, C.; Stoye, P. J.; Yap, W. M. *Proc. Natl. Acad. Sci.* **2004**, 101, 13324.
- Lanman, J.; Sexton, J.; Sakalian, M.; Prevelige, P. E. *J. Virol.* **2002**, 76, 6900.
- Luban, J. *Cell* **1996**, 87, 1157.
- Li, J.; Chen, J.; Zhang, L.; Wang, F.; Gui, C.; Zhang, L.; Qin, Y.; Xu, Q.; Liu, H.; Nan, F.; Shen, J.; Bai, D.; Chen, K.; Shen, X.; Jiang, H. L. *Bioorg. Med. Chem.* **2006**, 14, 5527.
- Liu, J.; Chen, C. M.; Walsh, C. T. *Biochemistry* **1991**, 30, 2306.
- Fischer, G.; Berger, E.; Bang, H. *FEBS Lett.* **1989**, 2, 267.
- Kofron, J. L.; Kuzmic, P.; Kishore, V.; Colon-Bonilla, E.; Rich, H. D. *Biochemistry* **1991**, 30, 6127.
- Thaddeus, A. T.; Victoria, W. M.; Heidi, G. B.; Michael, L. M.; Thomas, D. M. *Biochem. Biophys. Res. Commun.* **1990**, 168, 264.
- Timothy, M. J.; Alan, E.; Rodolfo, G.; Rebort, C. *J. Biol. Chem.* **1996**, 271, 7712.
- Daria, J. H.; Jeffrey, C. H.; Abigail, L. W.; Emilio, A. E. *Nucleic Acids. Res.* **1994**, 22, 1121.
- Pettersen, E. F.; Goddard, T. D.; Huang, C. C.; Couch, G. S.; Greenblatt, D. M.; Meng, E. C.; Ferrin, T. E. *J. Comput. Chem.* **2004**, 25, 1605.
- Gershon, H.; Grefig, A.; Clarke, D. D. *J. Heterocycl. Chem.* **1987**, 24, 205.
- Soai, K.; Yokoyama, S.; Mochida, K. *Synthesis* **1987**, 7, 647.
- Katritzky, A. R.; Ji, F. B.; Fan, W. Q.; Beretta, P.; Bertoldi, M. *J. Heterocycl. Chem.* **1992**, 29, 1519.
- Hazuda, J. D.; Felock, P.; Witmer, M.; Wolfe, A.; Stillmock, K.; Grobler, A. J.; Espeseth, A.; Gabryelski, L.; Schleif, W.; Blau, C.; Miller, D. M. *Science* **2000**, 287, 646.
- Kallen, J.; Spitzfaden, C.; Zurini, M. M.; Wider, G.; Widmer, H.; Wuthrich, K.; Walkshaw, M. *Nature* **1991**, 353, 276.